Surface-emitting quantum-cascade lasers with a grating formed by focused ion beam milling

© A.V. Babichev[1], D.A. Mikhailov[2], E.S. Kolodeznyi[1], A.G. Gladyshev[1], G.V. Voznyuk[2], M.I. Mitrofanov[2,3], D.V. Denisov[4], S.O. Slipchenko[2], A.V. Lyutetskii[2], V.V. Dudelev[2], V.P. Evtikhiev[2], L.Yu. Karachinsky[1], I.I. Novikov[1], G.S. Sokolovskii[2], N.A. Pikhtin[2], A.Yu. Egorov[5]

[1] ITMO University,
197101 St. Petersburg, Russia
[2] Ioffe Institute,
194021 St. Petersburg, Russia
[3] Submicron Heterostructures for Microelectronics, Research and Engineering Center,
Russian Academy of Sciences,
194021 St. Petersburg, Russia
[4] St. Petersburg State Electrotechnical University „LETI",
197022 St. Petersburg, Russia
[5] Alferov Federal State Budgetary Institution of Higher Education and Science
Saint Petersburg National Research Academic University of the Russian Academy of Sciences,
194021 St. Petersburg, Russia

E-mail: a.babichev@mail.ioffe.ru

Received April 18, 2022
Revised June 25, 2022
Accepted July 5, 2022

The results of studies of $7.5-8.0\,\mu$m range surface-emitting ring quantum-cascade lasers are presented. A second-order diffraction grating with a calculated coupling coefficient of $\sim 9\,\mathrm{cm}^{-1}$ is formed on the entire surface of the ring cavity by focused ion beam milling. Surface-emitting lasing at room temperature near $7.75\,\mu$m with a threshold current density of $\sim 8\,\mathrm{kA/cm}^2$ and an outer radius of the ring cavity of $202\,\mu$m is demonstrated. The results of studying the intensity distribution in the far-field near the normal to the surface showed the presence of two maxima. It is shown that the implemented coupling coefficient is not sufficient to ensure single-mode lasing in the studied ring quantum-cascade lasers.

Keywords: superlattices, quantum-cascade laser, epitaxy, indium phosphide, focused ion beam milling.

DOI: 10.21883/SC.2022.09.54136.9857

1. Introduction

Next-generation chemical fingerprinting systems [1,2] require the development of sources and detectors of radiation of the long-wave infrared spectral range. Quantum-cascade lasers (QCLs) and quantum-cascade detectors are of interest in the context of design of such systems, since they may be integrated on a single chip [3,4] to fabricate both gas sensors and microfluidic sensors [5].

The use of a ring cavity combined with the formation of a second-order diffraction grating in layers of the top waveguide cladding allows for surface emission [6]. Owing to the lack of additional optical losses at mirrors that are typical of stripe lasers, this approach was the first to enable surface lasing under continuous current pumping at room temperature with an output optical power of $\sim 0.5\,\mathrm{W}$ [7,8]. Frequency combs operating under continuous current pumping were produced by applying the technique of regrowth of semi-insulating indium phosphide to a ring cavity [9–11].

The typical far field of a QCL with a ring cavity has the form of concentric rings with an intensity minimum at the center and azimuthal polarization of radiation [7]. In certain applications, the intensity needs to be maximized at the center of the far field. Several approaches to generating an intensity maximum at the center of the far field of a QCL with a ring cavity have been proposed. Among them are the implementations of two abrupt π phase shifts spaced apart by 180° [12–14]; a grating offset in the horizontal plane by $\Lambda/4$, where Λ is the diffraction grating period [15]; a rotation of the grating grooves [15]; a double diffraction grating with the inner grating shifted by π relative to the outer one [16]; and flat lenses integrated monolithically on a substrate via the formation of metamaterial layers with a refraction index gradient [13,16].

This paper presents the first results of studies into the fabrication and examination of a QCL with a ring cavity with a second-order diffraction grating formed throughout the entire length of the cavity by focused ion beam milling. The design with a double abrupt phase shift by π was utilized [12–14].

2. Experimental samples

Molecular beam epitaxy (MBE) was used to form a multiperiod QCL heterostructure [17]. The epitaxy of cascade layers, which were fabricated based on a mechanically unstressed (with respect to the InP substrate)

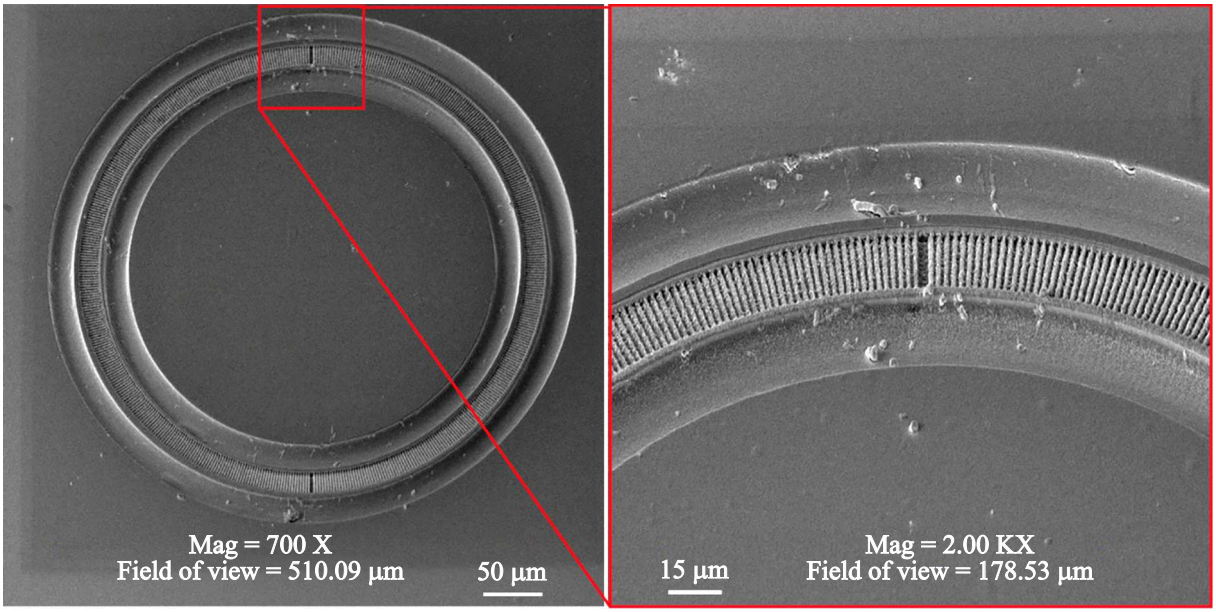

Figure 1. SEM image of a QCL with a ring cavity. The overall view is on the left, and the magnified image of the phase shift region is on the right.

$In_{0.53}Ga_{0.47}As/Al_{0.48}In_{0.52}As$ heteropair, was performed on an indium phosphide substrate following the formation of a buffer $In_{0.53}Ga_{0.47}As$ ($0.5\,\mu$m) layer. The ejection of carriers into the next period of an active region was implemented in the arrangement with two-phonon depletion of the lower level. The active region had 50 identical periods with a thickness of 52.7 nm. An InP layer with a thickness of $3.9\,\mu$m and a silicon concentration of $1.0 \cdot 10^{17}\,cm^{-3}$ was used to form the top waveguide cladding. $In_{0.53}Ga_{0.47}As$ layers with an overall thickness of 120 nm and a near-surface silicon concentration of $1.0 \cdot 10^{19}\,cm^{-3}$ were used as contact ones. A double-trench mesa design [18–20] was used in the fabrication of ring cavity crystals.

The outer radius of the ring cavity near the surface measured using the SEM image presented in Fig. 1 was $202\,\mu$m. The width of the ring cavity was $26\,\mu$m. The laser crystal was mounted with the substrate facing down onto a copper heat sink and soldered with indium solder. A diffraction grating was etched throughout the entire length of the cavity in ultra-high vacuum by a focused gallium beam with an ion energy of 30 keV and an operating current of 2000 pA [21].

The ion dose in etching of diffraction grating grooves was $1.4 \cdot 10^{11}\,pC/cm^2$. The diffraction grating period in angular coordinates was 0.72° (this corresponds to period $\Lambda = 2.375\,\mu$m for a ring cavity with length is $L = 1.188$ mm). The duty ratio was 50%. The depth of groove etching in heterostructure layers was 600 ± 50 nm (1200 ± 50 nm if the metallization thickness is taken into account). Coupling coefficient κ calculated for this diffraction grating within the coupled-mode theory [22], which is applicable in the case of small variations of the real part of the refraction index, was $\sim 9\,cm^{-1}$ ($\kappa L \approx 1$). This agrees with the results of experiments on single-frequency generation presented earlier ($\sim 8\,cm^{-1}$, $\kappa L \approx 1$ [23], $\kappa \sim 12\,cm^{-1}$, $\kappa L \approx 1.5$ [24]).

The width of etched grooves was doubled at tracking angles of 90 and 270° to implement a phase shift by π (see Fig. 1, right panel).

The QCL generation spectra were recorded with a Bruker Vertex 70v Fourier spectrometer with a spectral resolution of $0.2\,cm^{-1}$. The dependence of the emission intensity on the amplitude of pulsed current pumping was measured normally to the ring cavity plane at a distance of ~ 1 cm from a Thorlabs C036TME-E collecting lens. The pulse repetition rate was 8.5 kHz, and the pulse duration was 75 ns. The distributions of intensity in the near and far field and the lasing spectra were measured under pulsed pumping with a pulse repetition rate of 48 kHz and a pulse duration of 75 ns. The QCL heat sink temperature was 291 K in all experiments. The near field of the QCL with a ring cavity geometry was imaged with a bolometric Dataray WinCamD-IR-BB camera. The net optical magnification ratio of the system was 8.75. The distribution of laser emission intensity in the far field region was recorded without optical radiation collection systems using a Vigo PVI-4TE-10.6 photovoltaic detector mounted on a goniometer at a distance of 7 cm [25]. Lock-in detection was implemented to make the measurement system resistant to interference.

3. Results and discussion

The dependence of the integral emission intensity on the current pumping level is presented in Fig. 2, and a scanning electron microscopy (SEM) image is shown in

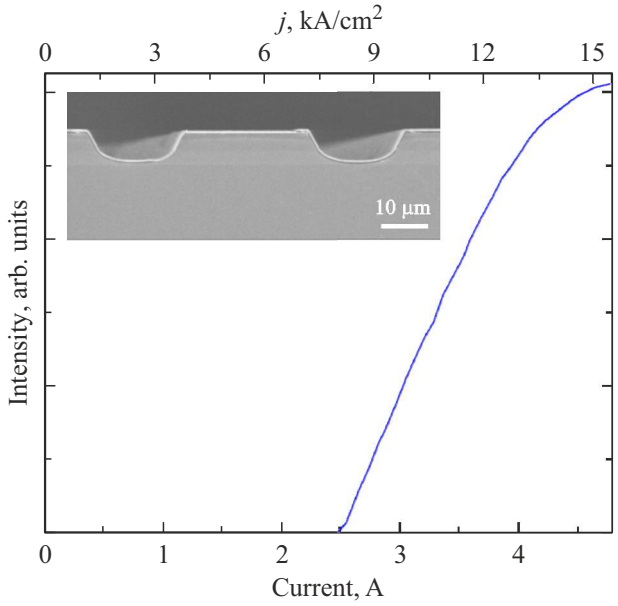

Figure 2. Dependence of the integral emission intensity on the current pumping level. A SEM image of a fragment of the cleavage surface of the QCL crystal with a ring cavity is shown in the inset. The formation of a mesa with a double trench is evident.

the inset of the same figure. Threshold current I_{th} was ~ 2.5 A, which corresponds to threshold current density $j_{\text{th}} \sim 8$ kA/cm^2. Thus, following the etching of a diffraction grating throughout the entire length of the ring cavity, the threshold current increased from 6.7 kA/cm^2 (see [20]) to 8.0 kA/cm^2. The watt–ampere characteristic reaches saturation at a current of $1.8I_{\text{th}}$. The total optical losses in the studied laser were estimated with account for differential gain $(g\Gamma) \approx 3.3$ cm/kA [20] (g is the differential gain and Γ is the optical limiting factor) of the considered heterostructure type and were found to be equal to $\alpha_{Ring} = j_{\text{th}} g\Gamma \approx 26\,\text{cm}^{-1}$. Taking the estimate of total internal losses for a QCL with a ring cavity without a diffraction grating ($22\,\text{cm}^{-1}$ [20]) into account, we found the optical losses associated with radiation outcoupling through grating layers: $\sim 4\,\text{cm}^{-1}$. Losses at mirrors α_m in a stripe laser with the same cavity length L were calculated as $\alpha_m = \ln(R_{\text{eff}})/L$, where $R_{\text{eff}} = (n_{\text{eff}} - 1)^2/(n_{\text{eff}} + 1)^2$ [20], and were estimated at $\sim 11\,\text{cm}^{-1}$. Thus, the radiation outcoupling losses in a ring cavity are almost 3 times lower than the losses in half-ring lasers with the same cavity length. Apparently, this is attributable to the fact that grating grooves are etched to a shallow depth.

The surface lasing spectra are presented in Fig. 3. The lasing spectrum features five lines corresponding to five azimuthal modes around 7.75 μm and thus differs from the spectrum in [6] with 40 azimuthal modes. At the same time, single-frequency generation (similar to the one reported in [7]) was not achieved, which is apparently attributable to an insufficient coupling coefficient. It has already been demonstrated [26] that single-mode lasing may probably be achieved with such grating parameters at lower temperatures, but a higher coupling coefficient is required for single-mode lasing at room temperature.

The group refraction index was estimated based on the intermode distance for whispering-gallery modes: $n_{\text{gr}} = 3.39$.

If we assume that the optical mode with a wavelength of 7.743 μm is the fundamental one, expression $n_{\text{eff}}(\lambda) = \lambda/\Lambda$ yields effective refraction index $n_{\text{eff}} = 3.26$. Using the $n_{\text{gr}} = n_{\text{eff}}(\lambda) - \lambda dn_{\text{eff}}(\lambda)/d\lambda$ expression, we determine the quantity characterizing the dispersion of refraction index: $dn_{\text{eff}}(\lambda)/d\lambda = 0.0167\,\mu\text{m}^{-1}$. When the current pumping level reaches 4 A, the intensity of higher-order modes increases, and the modes get shifted toward longer wavelengths in the spectrum.

The magnitude of heating of the laser was estimated based on this shift of individual modes. Taking the value of $\Delta\lambda/\Delta T = 0.56$ nm/K [27] into account, we estimated that the laser was heated by $\sim 6^\circ$C in the transition to a pumping level of 4 A.

The results of examination of the intensity distribution in the near field region are presented in Fig. 4. At a pumping current of 2.5 A, the near-field intensity distribution corresponds to the ring cavity (the grating region through

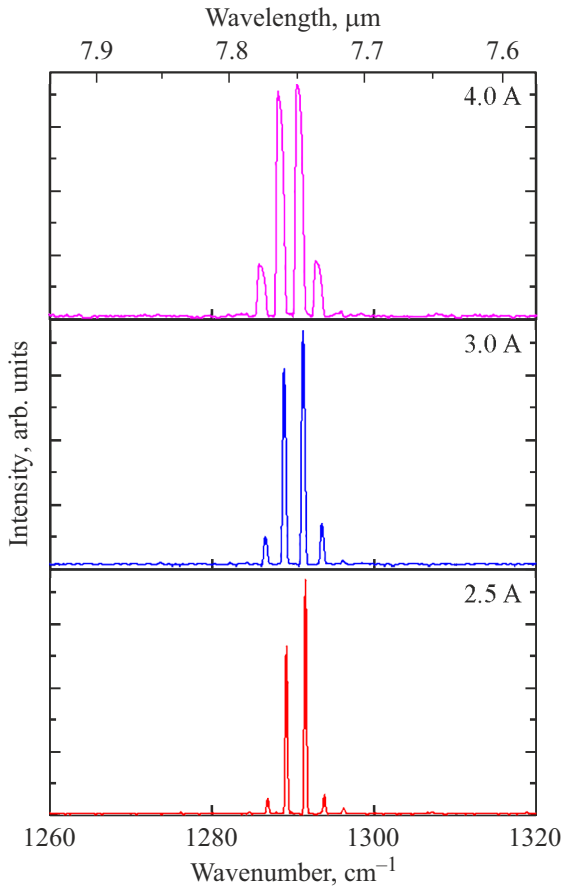

Figure 3. Surface lasing spectra of ring QCLs (with normalized intensity) measured at different levels of current pumping.

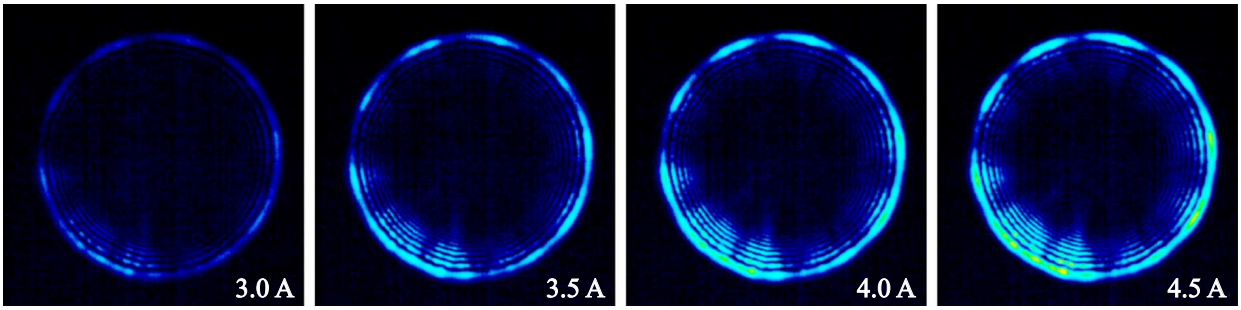

Figure 4. Intensity distributions in the near field region at different levels of current pumping.

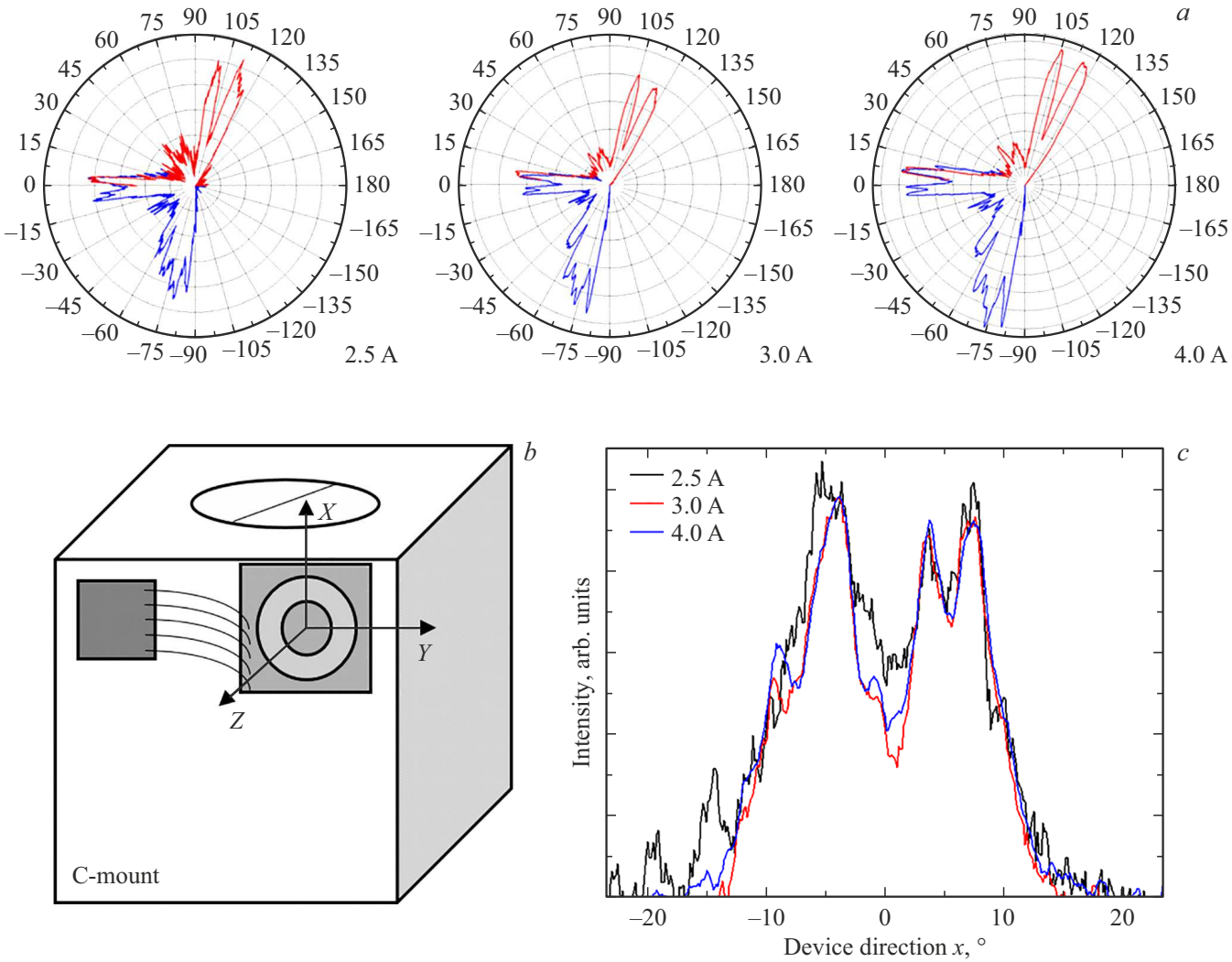

Figure 5. *a* — Distributions of *XZ* intensity in the far field region at different levels of current pumping; *b* — schematic diagram of the sample positioning on a C-mount heat sink and the orientation of axes *XYZ*; *c* — normalized *XZ* intensity distributions in the far filed region around the surface normal. (A color version of the figure is provided in the online version of the paper).

which radiation is outcoupled). The nonuniformity of intensity at different azimuthal angles is worth noting. This effect has been observed earlier in [12] and may be attributed either to nonuniform current pumping or to the nonuniformity of the etching depth along the ring cavity. Just like in [1,12,15,16,28], additional smaller interference rings are observed in addition to the emission intensity corresponding to the ring cavity radius. An intensity maximum at the center of interference rings produced due to reflection from lenses (see [1] was not found.

Additional near-field measurements with radiation passing through a linear polarizer [7,12,16] should help verify that the light polarization is azimuthal [29].

The results of examination of the intensity distribution in the far field region in plane XZ are shown in Fig. 5. The schematic diagram of the sample positioning on a heat sink and the orientation of axes XYZ is presented in Fig. 5, *b*. Three lobes are seen in the radiation pattern: one normal to the sample surface (around 0°) and two lobes corresponding to radiation with outcoupling angles near -75° and 110°.

The far-field intensity distribution around 0°, which corresponds to the surface normal, features two maxima. This agrees with the data reported in [6] and is the result of multimode lasing. The FWHM of the far-field intensity distribution was $\sim 20^\circ$ ($1/e^2 \approx 25^\circ$). In single-mode lasing, the far field should have the form of a set of diffraction concentric rings [30] with a diffraction fringe distance defined by expression $\sin(2\Theta) = (k + m/2)\lambda/R$ [7], where R is the ring cavity radius, k is the diffraction order, and m is the number of the azimuthal mode at which lasing is observed. In the case of fundamental-mode lasing, the estimated diffraction fringe distance for the studied QCL is 1.2°. However, the variation of radiation outcoupling angles corresponding to different modes leads to diffusion of the far field in the experimentally observed multimode lasing regime. Azimuthal radiation outcoupling angle $\alpha = \arcsin(n_{\text{eff}} - \lambda/\Lambda)$, where Λ is the wavelength of the optical mode [31], varies within 1.4° for five lasing lines presented in Fig. 3. Therefore, it is impossible to estimate, following [7,30], the order of the fundamental mode at which lasing is observed. Radiation with an outcoupling angle near -75° is emitted from the end face of the QCL crystal, since lasing proceeds not only in the vertical direction, but also in the QCL crystal plane. The lobe around 110° represents, in turn, a combination of rereflection of QCL radiation from the heat sink surface superimposed on shading of radiation from an insulating contact pad mounted on the heat sink.

4. Conclusion

A QCL with a ring cavity with a diffraction grating formed throughout the entire length of the cavity by focused ion beam milling was examined. Surface lasing around $7.75\,\mu$m at room temperature was demonstrated. The level of optical losses associated with radiation outcoupling through the diffraction grating was estimated at $\sim 4\,\text{cm}^{-1}$.

The examination of radiation intensity in the far field region revealed that coupling coefficient $\kappa \sim 9\,\text{cm}^{-1}$ ($\kappa L \approx 1$) of the diffraction grating is not sufficient to achieve single-frequency lasing. An over-coupling regime with $\kappa L \approx 10$ [31] needs to be established in future experiments. According to numerical estimates, this requires increasing the etching depth of grating grooves to $3.4\,\mu$m. The use of a diffraction grating with metal-coated grooves should help reduce the etching depth [8], but will require the application of the Floquet–Bloch theory in calculations of coupling in gratings with a significant jump in refraction index [32,33]. The application of this approach is, in turn, associated with a considerable increase in optical losses (due to the presence of metallization on the surface of etched grooves) and may eventually lead to additional growth of the threshold current of a ring QCL.

Funding

This study was supported financially by a grant from the Russian Science Foundation (project No. 20-79-10285).

Conflict of interest

The authors declare that they have no conflict of interest.

References

[1] A. Harrer, R. Szedlak, B. Schwarz, H. Moser, T. Zederbauer, D. MacFarland, H. Detz, A.M. Andrews, W. Schrenk, B. Lendl, G. Strasser. Sci. Rep., **6** (1), 1 (2016).
[2] F. Kapsalidis, M. Shahmohammadi, M.J. Süess, J.M. Wolf, E. Gini, M. Beck, M. Hundt, B. Tuzson, L. Emmenegger, J. Faist. Appl. Phys. B, **124** (6), 1 (2018).
[3] R. Szedlak, J. Hayden, P. Martín-Mateos, M. Holzbauer, A. Harrer, B. Schwarz, B. Hinkov, D. MacFarland, T. Zederbauer, H. Detz, A.M. Andrews, W. Schrenk, P. Acedo, B. Lendl, G. Strasser. Opt. Eng., **57** (1), 011005 (2017).
[4] R. Szedlak, A. Harrer, M. Holzbauer, B. Schwarz, J.P. Waclawek, D. MacFarland, T. Zederbauer, H. Detz, A. M. Andrews, W. Schrenk, B. Lendl, G. Strasser. ACS Photonics, **3** (10), 1794 (2016).
[5] B. Hinkov, H. Knötig, F. Pilat, S. Lindner, R. Weih, B. Schwarz, W. Schrenk, L. Lux, H. Detz, A.M. Andrews, B. Baumgartner, J.P. Waclawek, J. Koeth, S. Höfling, B. Lendl, G. Strasser. *Mid-infrared lasers for spectroscopic applications. 1st Global Infrared Sessions.* https://publik.tuwien.ac.at/files/publik_301887.pdf
[6] E. Mujagić, S. Schartner, L.K. Hoffmann, W. Schrenk, M.P. Semtsiv, M. Wienold, W.T. Masselink, G. Strasser. Appl. Phys. Lett., **93** (1), 011108 (2008).
[7] Y. Bai, S. Tsao, N. Bandyopadhyay, S. Slivken, Q. Y. Lu, D. Caffey, M. Pushkarsky, T. Day, M. Razeghi. Appl. Phys. Lett., **99** (26), 261104 (2011).
[8] D.H. Wu, M. Razeghi. APL Mater., **5** (3), 035505 (2017).
[9] B. Meng, M. Singleton, M. Shahmohammadi, F. Kapsalidis, R. Wang, M. Beck, J. Faist. Optica, **7** (2), 162 (2020).
[10] D. Kazakov, N. Opačak, M. Beiser, A. Belyanin, B. Schwarz, M. Piccardo, F. Capasso. Optica, **8** (10), 1277 (2021).
[11] B. Meng, M. Singleton, J. Hillbrand, M. Franckié, M. Beck, J. Faist. Nature Photonics, **16** (2), 142 (2022).
[12] C. Schwarzer, R. Szedlak, S.I. Ahn, T. Zederbauer, H. Detz, A.M. Andrews, W. Schrenk, G. Strasser. Appl. Phys. Lett., **103** (8), 081101 (2013).
[13] R. Szedlak, M. Holzbauer, P. Reininger, D. MacFarland, T. Zederbauer, H. Detz, A.M. Andrews, W. Schrenk, G. Strasser. Vib. Spectrosc., **84**, 101 (2016).

[14] J.-C. Zhang, D.-Y. Yao, N. Zhuo, F.-L. Yan, F.-Q. Liu, L.-J. Wang, J.-Q. Liu, Z.-G. Wang. Appl. Phys. Lett., **104** (5), 052109 (2014).
[15] R. Szedlak, C. Schwarzer, T. Zederbauer, H. Detz, A.M. Andrews, W. Schrenk, G. Strasser. Opt. Express, **22** (13), 15829 (2014).
[16] R. Szedlak, M. Holzbauer, D. MacFarland, T. Zederbauer, H. Detz, A.M. Andrews, C. Schwarzer, W. Schrenk, G. Strasser. Sci. Rep., **5** (1), 16668 (2015).
[17] A.Yu. Egorov, A.V. Babichev, L.Ya. Karachinsky, I.I. Novikov, E.V. Nikitina, M. Tchernycheva, A.N. Sofronov, D.A. Firsov, L.E. Vorobjev, N.A. Pikhtin, I.S. Tarasov. Semiconductors, **49** (11), 1527 (2015).
[18] M. Piccardo, B. Schwarz, D. Kazakov, M. Beiser, N. Opačak, Y. Wang, S. Jha, J. Hillbrand, M. Tamagnone, W.T. Chen, A.Y. Zhu, L.L. Columbo, A. Belyanin, F. Capasso. Nature, **582** (7812), 360 (2020).
[19] A.V. Babichev, A.G. Gladyshev, A.S. Kurochkin, V.V. Dudelev, E.S. Kolodeznyi, G.S. Sokolovskii, V.E. Bugrov, L.Ya. Karachinsky, I.I. Novikov, D.V. Denisov, A.S. Ionov, S.O. Slipchenko, A.V. Lyutetskii, N.A. Pikhtin, A.Y. Egorov. Techn. Phys. Lett., **45** (4), 398 (2019).
[20] A.V. Babichev, D.A. Pashnev, A.G. Gladyshev, A.S. Kurochkin, E.S. Kolodeznyi, L.Ya. Karachinsky, I.I. Novikov, D.V. Denisov, V.V. Dudelev, G.S. Sokolovskii, D.A. Firsov, L.E. Vorob'ev, S.O. Slipchenko, A.V. Lutetskiy, N.A. Pikhtin, A.Y. Egorov. Opt. Spectrosc., **128** (8), 1187 (2020).
[21] A.V. Babichev, E.S. Kolodeznyi, A.G. Gladyshev, D.V. Denisov, G.V. Voznyuk, M.I. Mitrofanov, N.Yu. Kharin, V.Yu. Panevin, S.O. Slipchenko, A.V. Lyutetskii, V.P. Evtikhiev, L.Ya. Karachinsky, I.I. Novikov, N.A. Pikhtin, A.Yu. Egorov. Semiconductors, **55** (7), 591 (2021)].
[22] H. Kogelnik, C.V. Shank. J. Appl. Phys., **43** (5), 2327 (1972).
[23] E. Mujagić, L.K. Hoffmann, S. Schartner, M. Nobile, W. Schrenk, M.P. Semtsiv, M. Wienold, W.T. Masselink, G. Strasser. Appl. Phys. Lett., **93** (16), 161101 (2008).
[24] E. Mujagić, C. Schwarzer, Y. Yao, J. Chen, C. Gmachl, G. Strasser. Appl. Phys. Lett., **98** (14), 141101 (2011).
[25] V.V. Dudelev, S.N. Losev, V.Yu. Mylnikov, A.V. Babichev, E.A. Kognovitskay, S.O. Slipchenko, A.V. Lutetskii, N.A. Pikhtin, A.G. Gladyshev, L.Ya. Karachinskii, I.I. Novikov, A.Yu. Egorov, V.I. Kuchinskii, G.S. Sokolovskii. Opt. Spectrosc., **125** (3), 402 (2018).
[26] C. Schwarzer, E. Mujagić, S.I. Ahn, A.M. Andrews, W. Schrenk, W. Charles, C. Gmachl, G. Strasser. Appl. Phys. Lett., **100** (19), 191103 (2012).
[27] A.V. Babichev, E.S. Kolodeznyi, A.G. Gladyshev, D.V. Denisov, N.Yu. Kharin, A.D. Petruk, V.Yu. Panevin, S.O. Slipchenko, A.V. Lyutetskii, L.Ya. Karachinsky, I.I. Novikov, N.A. Pikhtin, A.Yu. Egorov, Tech. Phys. Lett., **48** (3), 6 (2022).]
[28] C. Schwarzer, R. Szedlak, L. Burgstaller, A. Genner, T. Zederbauer, H. Detz, A.M. Andrews, W. Schrenk, G. Strasser. „Polarization versatility of surface emitting ring cavity quantum cascade lasers", in *2013 Conf. on Lasers & Electro-Optics Europe & International Quantum Electronics Conf. CLEO EUROPE/IQEC* (Munich, Germany, May 2013). DOI: 10.1109/cleoeiqec.2013.6800693
[29] M. Holzbauer, R. Szedlak, H. Detz, R. Weih, S. Höfling, W. Schrenk, J. Koeth, G. Strasser. Appl. Phys. Lett., **111** (17), 171101 (2017).
[30] E. Mujagić, M. Nobile, H. Detz, W. Schrenk, J. Chen, C. Gmachl, G. Strasser. Appl. Phys. Lett., **96** (3), 031111 (2010).
[31] B.G. Lee, H.A. Zhang, C. Pflugl, L. Diehl, M.A. Belkin, M. Fischer, A. Wittmann, J. Faist, F. Capasso. IEEE Phot. Techn. Lett., **21** (13), 914 (2009).
[32] N. Finger, W. Schrenk, E. Gornik. IEEE J. Quant. Electron., **36** (7), 780 (2000).
[33] H. Shu, M. Suttinger, A. Lyakh. IEEE J. Quant. Electron., **55** (1), 1 (2019).